



Representation of thermal information in the antennal lobe of leaf-cutting ants

Markus Ruchty^{1,2}, Fritjof Helmchen², Rüdiger Wehner² and Christoph Johannes Kleineidam^{1,3*}

¹ Department of Behavioral Physiology and Sociobiology, Biozentrum, University of Würzburg, Würzburg, Germany

² Department of Neurophysiology, Brain Research Institute, University of Zürich, Zürich, Switzerland

³ Department of Biology, University of Konstanz, Konstanz, Germany

Edited by:

Riccardo Brambilla, San Raffaele Scientific Institute and University, Italy

Reviewed by:

Jean-Christophe Sandoz, Centre National de la Recherche Scientifique, France

Wulfila Gronenberg, University of Arizona, USA

*Correspondence:

Christoph Johannes Kleineidam, Department of Biology, University of Konstanz, Universitaetsstrasse 10, 78457 Konstanz, Germany.
e-mail: christoph.kleineidam@uni-konstanz.de

Insects are equipped with various types of antennal sensilla, which house thermosensitive neurons adapted to receive different parameters of the thermal environment for a variety of temperature-guided behaviors. In the leaf-cutting ant *Atta vollenweideri*, the physiology and the morphology of the thermosensitive sensillum coeloconicum (Sc) has been thoroughly investigated. However, the central projections of its receptor neurons are unknown. Here we selectively stained the three neurons found in single Sc and tracked their axons into the brain of *Atta vollenweideri* workers. Each of the three axons terminates in a single glomerulus of the antennal lobe (Sc-glomeruli). Two of the innervated glomeruli are adjacent to each other and are located laterally, while the third one is clearly separated and located medially in the antennal lobe. Using two-photon Ca²⁺ imaging of antennal lobe projection neurons, we studied where in the antennal lobe thermal information is represented. In the 11 investigated antennal lobes, we found up to 10 different glomeruli in a single specimen responding to temperature stimulation. Both, warm- and cold-sensitive glomeruli could be identified. The thermosensitive glomeruli were mainly located in the medial part of the antennal lobe. Based on the general representation of thermal information in the antennal lobe and functional data on the Sc-glomeruli we conclude that temperature stimuli received by Sc are processed in the medial of the three target glomeruli. The present study reveals an important role of the antennal lobe in temperature processing and links a specific thermosensitive neuron to its central target glomerulus.

Keywords: social insect, two-photon imaging, sensilla coeloconica, temperature processing

INTRODUCTION

Insects possess a highly developed thermal sense to assess various parameters of their thermal environment. Apart from temperature avoidance or preference required for successful thermoregulation of the own body temperature some insects utilize their thermal sense for amazingly sophisticated temperature-guided behaviors. For example blood-sucking bugs detect thermal radiation emitted by their endothermic prey to receive a blood meal (Lazzari and Núñez, 1989; Schmitz et al., 2000; Lazzari, 2009), Australian fire beetles locate forest fires to encounter mates and to reproduce (Evans, 1964; Vondran et al., 1995; Schmitz et al., 1997), and leaf-cutting ants can use thermal radiation as an orientation cue (Kleineidam et al., 2007). Most of the thermosensitive neurons that receive thermal information about the environment in insects are located on the antennae within cuticular structures termed peg-in-pit sensilla. These sensilla generally house three receptor neurons, combining one thermosensitive neuron with either two antagonistic hygroresponsive neurons (Waldow, 1970; Tichy, 1979; Altner et al., 1981; Altner and Loftus, 1985) or two chemosensitive neurons (Altner et al., 1977, 1981; Davis, 1977; Hansson et al., 1996). In social insects the thermo-hygroresponsive combination has been described for sensilla coelocapitula in the honeybee *Apis mellifera* (Yokohari, 1983). Other thermosensitive neurons have been found in sensilla ampullacea and the sensilla coeloconica (Lacher, 1964; Dumpert, 1978; Kleineidam and Tautz, 1996).

In the leaf-cutting ant *Atta vollenweideri* the sensilla coeloconica (Sc) have been studied in great detail. This sensillum is mainly located at the tip of the flagellum and has a remarkable peg-in-pit morphology where the sensory peg is deeply sunken in the cuticular pit, which is separated from the environment by a tiny aperture (Ruchty et al., 2009). The sensillum houses a thermosensitive (cold-sensitive) neuron presumably combined with two additional chemosensitive neurons (Ruchty et al., 2009). Recent electrophysiological investigations revealed an extreme sensitivity and high temporal resolution of the thermosensitive neuron (Ruchty et al., 2010). Based on the response characteristic to thermal stimuli and due to the extraordinary morphology of the sensillum, this neuron has been suggested as a candidate for detecting spatially distributed thermal objects during thermal landmark orientation (Kleineidam et al., 2007; Ruchty et al., 2009, 2010). In order to understand how insects orient in their thermal environment, it is necessary to know where and how thermal information is processed in the central nervous system. Until now, the central projections of thermosensitive neurons have been investigated only in a single study (Nishikawa et al., 1995). This tracing study nicely shows where thermal information of two specific thermosensitive neurons is further processed in the antennal lobe of the cockroach. However, it leaves unspecified where thermal information is represented within the whole antennal lobe volume.

In the present study we investigate the representation of thermal information in the antennal lobe of the leaf-cutting ant *Atta vollenweideri*. In particular, we focus on the thermal information received by the thermosensitive neuron of the Sc. Using two-photon Ca^{2+} imaging we measure the spatiotemporal neuronal activity upon temperature stimulation throughout the whole antennal lobe neuropil. By selectively staining single sensilla (Sc), we investigate the central projections of the receptor neuron axons into the ants' antennal lobes (Sc target glomeruli). Based on the correlation between the representation of thermal information within the antennal lobe and the Sc target glomeruli, we identify the target glomerulus of the thermosensitive neuron of the Sc.

MATERIALS AND METHODS

ANIMALS

Workers of *Atta vollenweideri* were obtained from a laboratory colony collected in 2002 at the Reserva Ecológica El Bagual, Formosa, Argentina. The colony was reared at the Biozentrum of the University of Würzburg at 25°C and 50% relative humidity in a 12-h/12-h photoperiod, and fed mainly with leaves of privet (*Ligustrum vulgare*) and dog rose (*Rosa canina*). The performed experiments comply with the current laws of the Federal Republic of Germany.

CENTRAL PROJECTIONS FROM SENSILLA COELOCONICA

We selectively stained single sensilla coeloconica (Sc) (single-staining) and investigated the anterograde projection of the receptor neuron axons into the ants' brains. Ants were mounted onto plexiglass holders with dental wax (surgident periphery wax, Heraeus Kulzer, Germany) and a strap of adhesive tape. Following the immobilization procedure, the scapus of each antenna was glued onto the holder by using white-out correction fluid (Tipp-Ex, Bic, France). Under visual control and at a magnification of 390 \times (Leitz microscope equipped with NPL-Fluotar L25/0.35, Leitz, Germany) an electrolytically sharpened tungsten electrode was inserted into a single Sc. The sensory peg was deliberately injured by carefully moving the electrode into the sensillum, which caused the permeation of receptor lymph into the chamber as observed under the microscope. The injured dendrites were then stained via a droplet of dextran-biotin (D-7135, Molecular Probes) dissolved in distilled water and applied onto the antennal tip for 10 min using a Hamilton syringe.

To investigate whether the target region in the ant's brain was exclusively innervated by receptor neuron axons of the Sc, we carried out a double-staining experiment. Subsequently to the single-staining we extensively cut antennal hair sensilla with a razorblade and stained the dendrites with tetra-methyl-rhodamine-dextran + biotin (3,000 MW, lysine-fixable; Microruby, D 7162, Molecular Probes) dissolved in distilled water.

All individuals from the single- and double-staining experiments were freed from the holders immediately after dye application and were kept separately in Petri dishes for the remaining staining period in order to avoid social grooming that could have decreased the staining success. After 24 h, the brains of the ants were dissected under ant saline solution (127 mM NaCl, 7 mM KCl, 1.5 mM CaCl_2 , 0.8 mM Na_2HPO_4 , 0.4 mM KH_2PO_4 , 4.8 mM

TES, 3.2 mM Trehalose, pH 7.0), transferred into ice-cold fixative (4% formaldehyde in phosphate buffered saline [PBS], pH 7.2), and stored overnight in the fridge. Brains were then rinsed in PBS (three times \times 10 min) and subsequently incubated in Alexa 488 conjugated streptavidin (S-11226, Molecular Probes, Eugene, OR) for 48 h. After being rinsed again in PBS (three times \times 10 min), the brains were dehydrated in an ascending ethanol series (50, 70, 90, 95, and three times 100%, \times 10 min), transferred into methyl-salicylate (M-2047, Sigma-Aldrich, Steinheim, Germany), and finally investigated under a confocal-laser-scanning microscope (Leica TSC SP 2, Leica Microsystems, Wetzlar, Germany). The software AMIRA 3.1 (Mercury Computer Systems, Berlin, Germany) was used to analyze the confocal image stacks (resolution: x : 0.3 μm ; y : 0.3 μm ; z : 1 μm) and to reconstruct the innervated neuropils as well as the axons of the labeled receptor neurons.

TWO-PHOTON Ca^{2+} IMAGING

Animal preparation

In order to study where in the antennal lobe thermal information is represented, we used a staining technique, which was already successfully used for calcium imaging in honeybees (Sachse and Galizia, 2002) and ants (Zube et al., 2008; Dupuy et al., 2010). We retrogradely labeled projection neurons that connect the antennal lobe via two antenno-protocerebral tracts (APTs) to the mushroom bodies and the lateral horn (Mobbs, 1982; Kirschner et al., 2006; Galizia and Rössler, 2010). The selective staining of projection neurons results in an excellent signal to noise ratio for two-photon Ca^{2+} imaging. Single ants were mounted in plexiglass holders using dental wax (surgident periphery wax, Heraeus Kulzer, Germany). Subsequently a small window was cut into the head capsule, and tracheae, glands, and muscles were gently moved aside in order to access the dye injection site in the lateral protocerebrum, close to the vertical lobe (alpha-lobe) of the right mushroom body. Prior to the dye injection a sharp glass electrode was used to perforate this region and to injure the projection neurons of the APTs. Afterward a second glass electrode coated with some crystals of Fura-2 dextran (potassium salt, 10000 MW, F3029, Molecular Probes) dissolved in distilled water was inserted in the perforated region and remained there for approximately 10 s. The brain was then covered by two-component glue (KWIK-SIL, World Precision Instruments, Berlin, Germany) to avoid desiccation, and the animals were kept in darkness for a staining period of around 3–4 h. Prior to the functional imaging experiments we first detached the KWIK-SIL from the brain. Then glands, tracheae, and muscles covering the antennal lobe ipsilateral to the injection site were removed. Subsequently, we excised the esophagus at the mouthparts, pulled it for a few millimeters out of the head capsule and fixated it with some dental wax next to the head capsule. This procedure was done to reduce brain movement during data acquisition. In order to protect the preparation and the brain, we again covered it with KWIK-SIL before mounting the plexiglass holder with the ant at the imaging setup.

Imaging setup

In vivo Ca^{2+} imaging was performed using a custom-built two-photon-laser-scanning microscope equipped with a Ti:sapphire laser system (MaiTai HP, Spectra-Physics, Newport, Santa Clara, USA) as light source (about 100 fs output). To excite the Fura-2 dye

we used a wavelength of 810 nm. The laser intensity was adjusted with a Pockel's cell (Conoptics, Danbury, USA). The microscope was equipped with two galvanometric scan mirrors (Model 6210; Cambridge Technologies, Lexington, USA) for scanning the specimen in the x - y axis, and a piezoelectric focusing element (P-725.4CD PIFOC, Physik Instrumente, Karlsruhe, Germany) for z -scanning along the optical axis. A water immersion objective (25 \times ; XPlan MP, 1.05 NA; Olympus) was mounted onto the piezo element, focusing the laser beam onto the antennal lobe and collecting the emitted fluorescence after dye excitation. To control the microscope and for data acquisition, custom-written software was used (LabView, National Instruments Corporation, Austin, TX, USA).

Odor and temperature stimuli

As a pre-test to check for vital preparation and successful staining procedure, we induced neuronal activity by stimulating the right antenna with two air puffs containing an odor mixture of citral and octanol (Aldrich Chemical Company, Inc.). The odors were loaded on a strip of filter paper (10 μ l of each odor at a concentration of 10^{-2} , with hexane as solvent; Aldrich Chemical Company, Inc.). After evaporation of the solvent for 4 min, the filter paper was placed into a syringe that was connected to a silicon tube used for stimulus application. The odor stimuli were applied manually 5 and 15 s after the recording was triggered.

Only those animals in which odor-elicited neuronal activity could be measured were subsequently used in the experiments designed to investigate the representation of thermal information within the antennal lobe. To generate warm (30°C) or cold (15°C) air stimuli, an airflow was channeled through a custom-made heat exchanger connected to a water bath via two silicon tubes (DC1, Haake, Germany, see Ruchty et al., 2010 for details). During both, odor and temperature stimulation a constant airflow (ca. 1.5 l/min) with stable room temperature of 24°C was blown over the preparation. The outlet of the stimulus air tube was positioned close to the ant's right antenna (2 cm distance) opposite to the continuous airflow. Temperature in both airflows was continuously measured by a thermocouple (ALMEMO, Ahlborn Messtechnik, Holzkirchen, Germany).

Optical recording of temperature-evoked neuronal activity

Functional data were collected by acquiring images with 128×128 pixel resolution and at a frame rate of 4 Hz. To screen the entire antennal lobe with all glomeruli for responses to temperature changes, we conducted 10–15 consecutive framescans (trials) in 10 μ m steps along the z -axis. In order to prevent neuronal adaptation in the thermosensitive neurons, we spaced the trials with a time interval of 2 min. During each trial the antenna was stimulated four times, every 20 frames (5 s) for a period of 2 s, by switching the stimulus airflow onto the antenna using a solenoid valve (Lee, USA) that was controlled by the data capture software. Having acquired the functional data, we recorded image stacks of the whole antennal lobe volume with a higher optical resolution (256 \times 256, 2 μ m step size).

Data processing and analysis

For data processing, the raw fluorescence images (frame scans) were read into NIH ImageJ. To calculate the relative change in fluorescence ($\Delta F/F$) we first subtracted the background fluorescence.

The mean of the first 20 images was used as reference (F_0) that was subtracted from each image in the sequence in order to obtain ΔF . The result (ΔF) was then divided by F_0 , which results in an image showing the relative fluorescence change ($\Delta F/F$). An increase in cytosolic Ca^{2+} , and thereby an increase in neuronal activity, causes a reduction in $\Delta F/F$ of the Fura-2 dye at an excitation wavelength of 810 nm (Grynkiewicz et al., 1985).

An average image of all frames of each trial (100 frames) was calculated and used to select regions of interest (ROI) that corresponded to single glomeruli. Every recognizable glomerulus at each scan-depth was labeled with an individual ROI, and the relative fluorescence change ($\Delta F/F$) over time (response kinetic) was analyzed. Apart from plotting the raw data traces, we visualized the changes in neuronal activity by calculating the average response during the four individual stimulus events. For this purpose the raw data image stack was sectioned into four substacks (each 25 frames long, e.g., frame 15–40 and frame 35–60) which were subsequently added and divided by 4. The relative change in fluorescence ($\Delta F/F$) was calculated similar to the raw data; except that F_0 was calculated as mean of the first five images of the four substacks (e.g., frame 15–20 or 35–40). In order to classify whether a glomerulus is thermosensitive or not, we first visually inspected the average traces looking for changes in $\Delta F/F$. Glomeruli which showed precise responses to stimulus on- and offset were assigned thermosensitive as soon as $\Delta F/F$ exceeded the threshold value of 4%, which is well above spontaneous changes in fluorescence. The resulting changes in relative fluorescence ($\Delta F/F$) could then be depicted as false color image sequence with blue and red indicating cold-sensitivity and warm-sensitivity of a glomerulus, respectively.

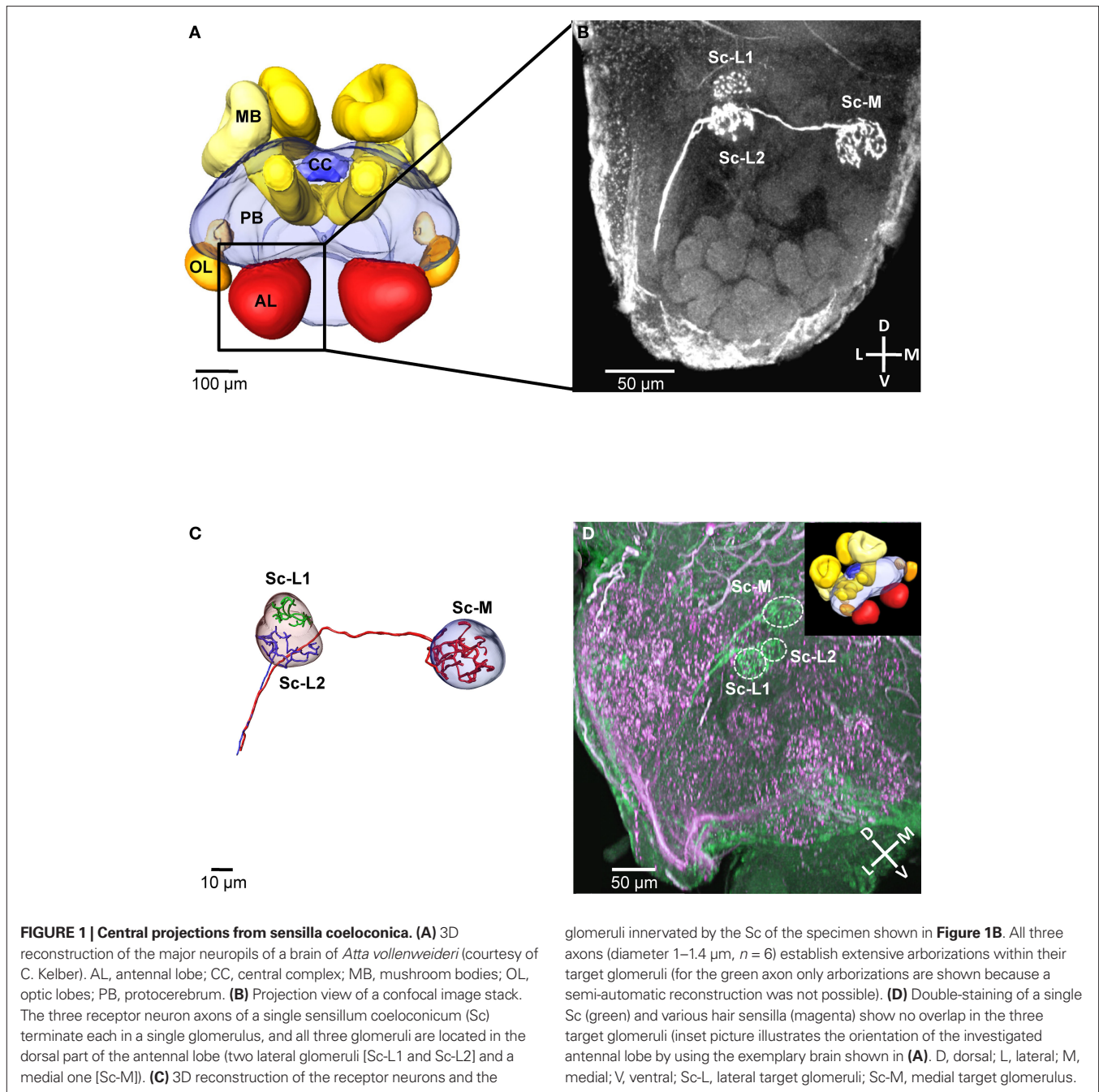
In order to map the position of thermosensitive glomeruli of different specimens in one common, averaged antennal lobe, we first moved the preparation in such a way that the anterior top of the antennal lobe in each specimen was centered. We then measured the x - y - z coordinates of every thermosensitive glomerulus in each of the investigated antennal lobes. In addition, we reconstructed an envelope of each antennal lobe, and by calculating the mean of all investigated antennal lobes ($n = 11$), we obtained a normalized antennal lobe. The 3D positions of the thermosensitive glomeruli were mapped, based on their normalized coordinates, into the normalized antennal lobe.

Changes in relative fluorescence of all responding and some non-responding glomeruli and the spatial representation of temperature stimuli were illustrated using ORIGIN 8.1 (OriginLab, USA) and Adobe Illustrator (Adobe, San Jose, USA). The 3D-reconstruction of glomeruli was accomplished by using the software AMIRA 5 (Mercury Computer Systems, Berlin, Germany).

RESULTS

CENTRAL PROJECTIONS FROM SENSILLA COELOCONICA

We selectively stained the receptor neurons of single sensilla coeloconica (Sc) in 19 independent preparations (antennae). In all of these cases, we found three receptor neuron axons, each innervating a single glomerulus in the same region within the ipsilateral antennal lobe (Example in **Figures 1A,B**). All three innervated glomeruli are located in the dorsal part of the antennal lobe, at a distance of 80–110 μ m (depth) from its anterior surface and close



to the dorsal lobe. Two of the innervated glomeruli are located at a lateral position, whereas the third glomerulus is located medially and is larger than the adjacent glomeruli in this region (**Figure 1B**). Because of their side-by-side position we termed the two lateral glomeruli Sc-L1 and Sc-L2 and later used them as landmarks. The medial glomerulus Sc-M, we could not use as a landmark because similar arrangements with a larger glomerulus are found in the dorsal part of the antennal lobe. This makes an unambiguous identification impossible.

All three neurons of a Sc have axons with a large diameter (mean = 1.12 μm , SD = 0.089; $n = 6$, measured at the unbranched axon after reconstruction, using the AMIRA measuring tool),

branch within the glomeruli and densely innervate the whole glomerular lumen (**Figures 1B,C**). The diameters of these receptor neuron axons are significantly larger in comparison to the axons of olfactory hair sensilla (mean = 0.62 μm , SD = 0.049, $n = 8$, $p < 0.01$; t -test). However, the shape and the size of the three glomeruli are similar to adjacent, putatively olfactory glomeruli (**Figure 1D**). Double-staining of receptor neuron axons from Sc (green) and from different types of hair sensilla (magenta) revealed that their glomerular innervation patterns do not overlap within the three Sc-glomeruli (double-staining: $n = 3$, **Figure 1D**). Thus, we conclude that the receptor neurons associated with Sc exclusively innervate the three Sc glomeruli.

TWO-PHOTON Ca^{2+} IMAGING

In 257 out of 810 investigated animals, projection neurons from the two APTs could be stained successfully. Two-photon image stacks through the antennal lobes (ipsilateral to the injection site) revealed that in the successful attempts the overall majority of glomeruli was stained with calcium sensitive dye and thus amenable for functional imaging (Figure 2A). The spatial resolution of the obtained image stacks is exceptional in all three spatial dimensions and enables the reconstruction of single glomeruli or of the whole antennal lobe in 3D, on the basis of *in vivo* morphological data (Figures 2A,B). Landmarks like the macroglomerulus (Kleineidam et al., 2005; Kuebler et al., 2010) or the antennal nerve and its tracts within the antennal lobes can be used to locate the area where the receptor neurons of the Sc terminate. Based on their position within the antennal lobe and their characteristic shape and arrangement, the two Sc-L glomeruli can be identified and serve as landmark glomeruli to localize the potential location of the Sc-M glomerulus. The example in Figure 2B depicts the positions of the three glomeruli that are putatively innervated by receptor neuron axons of the Sc (solid spheres).

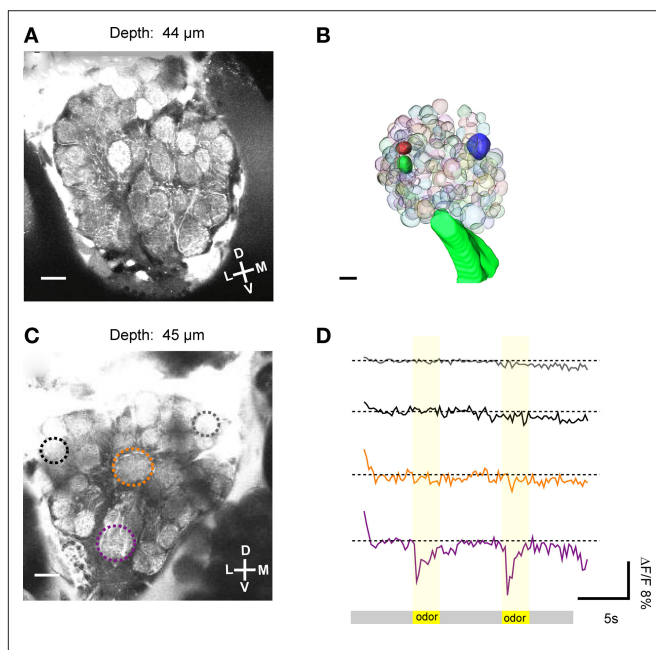


FIGURE 2 | Two-photon imaging of antennal lobe projection neurons.

(A) Based on the good optical resolution of the images obtained with the two-photon microscope, single glomeruli could be discriminated, some landmark glomeruli could be identified and neuronal activity could be measured selectively. (B) 3D reconstruction of single glomeruli in the antennal lobe based on *in vivo* morphological data. Individual glomeruli, in this case the three glomeruli that are putatively innervated by the receptor neuron axons of the sensilla coeloconica (Sc), could be identified (solid glomeruli). (C) The average image (100 frames) of a Ca^{2+} imaging trial was used to select regions of interest (ROI, encircled by dotted lines). The relative fluorescence change ($\Delta F/F$) in single glomeruli (ROIs) was measured upon stimulation. (D) In this optical section (depth = 45 μm), one glomerulus (purple ROI) responded to odor stimulation (two air puffs of a mixture of 10^{-2} citral and 10^{-2} octanol at second 5 and 15 of the recording) with a drop in $\Delta F/F$ of about 11%. Other glomeruli, e.g., the orange ROI did not respond to the odor stimulation. D, dorsal; L, lateral; M, medial; V, ventral. Scale: 10 μm .

In a total of 20 specimens we recorded odor evoked neuronal activity, as indicated by a sudden drop in fluorescence ($\Delta F/F$), which could be assigned to individual glomeruli of the antennal lobe. As an example, in Figure 2C an average image (100 recording frames) of an optical section through the antennal lobe is shown (depth = 45 μm). Upon stimulation with the odor mixture (10^{-2} citral and 10^{-2} octanol), one glomerulus responds strongly with an increase in neuronal activity.

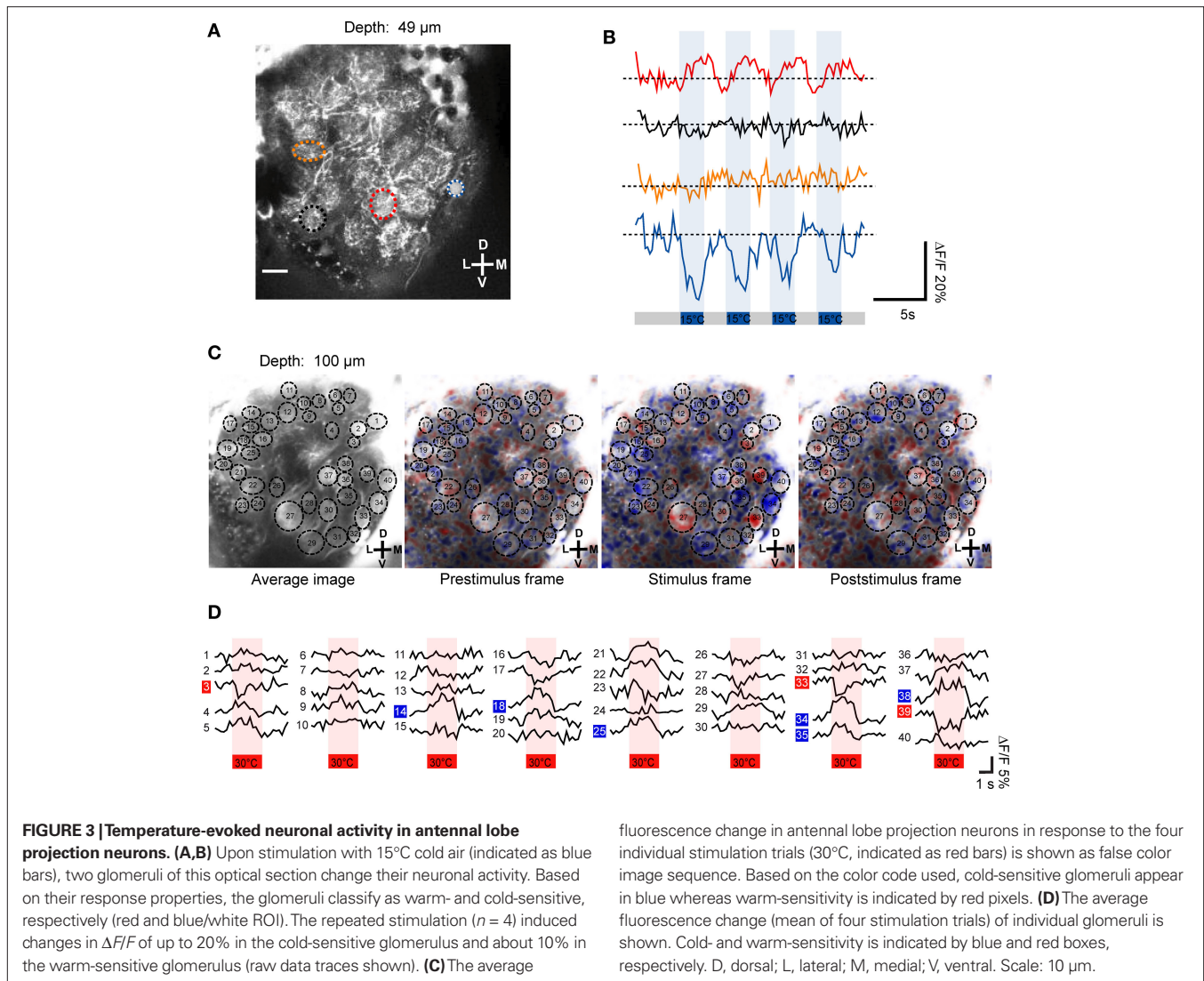
The resulting increase in cytosolic Ca^{2+} concentration in the projection neurons leads to a rapid (within one frame) drop in fluorescence ($\Delta F/F \approx 11\%$; purple ROI and purple trace; Figure 2D). The other glomeruli in the same optical section do not respond to this odor mixture.

Temperature-evoked neuronal activity in antennal lobe projection neurons

Using two-photon microscopy we screened the whole antennal lobe and investigated where thermal information is represented. In 11 specimens we successfully recorded changes in neuronal activity within antennal lobe glomeruli in response to temperature stimuli. By using repeated stimulation with temperature steps, both, warm- and cold-sensitive glomeruli, could be identified. In the example of Figures 3A,B the fluorescent changes in response to repeated cold stimulation ($15^\circ C$, $n = 4$) are visualized as raw data traces (depth = 49 μm). Two glomeruli respond to cold stimulation (step change to $15^\circ C$; ambient temperature = $24^\circ C$) with different response properties. The medial glomerulus (blue/white ROI and blue trace in Figures 3A,B) responds with a drop in fluorescence upon stimulation (cold-sensitive glomerulus). In contrast, a central glomerulus (red ROI and red trace in Figures 3A,B) seemed to be inhibited during the cold-stimuli and responded with increased activity after termination of the cold-stimuli (warm-sensitive glomerulus). There is a stronger Ca^{2+} signal in response to the temperature change in the cold-sensitive glomerulus ($\Delta F/F \approx 20\%$) than in the warm-sensitive glomerulus ($\Delta F/F \approx 10\%$). In Figure 3C the average response to four warm stimuli ($30^\circ C$) is shown as false color image sequence (depth = 100 μm). Cold-sensitive glomeruli appear in blue, whereas red indicates warm-sensitive glomeruli (Figure 3C). Based on our criteria used to analyze the data, three warm-sensitive glomeruli and six cold-sensitive glomeruli can be detected within this example. The response kinetics of the individual glomeruli vary to some extent. For example, they exhibit different response latencies to the stimulus application (Figure 3D). The changes in relative fluorescence seem sometimes to be rapid, step-like (e.g., ROI 33, 34 or ROI 39), and sometimes the maximum change is reached considerably more slowly, e.g., in ROI 14.

Spatial distribution of temperature-evoked neuronal activity

Across all 11 investigated specimens, we detected between 1 and 10 thermosensitive glomeruli per antennal lobe (median: 4 glomeruli). Among the 47 thermosensitive glomeruli we investigated in total, the majority ($n = 40$) respond with an increase in neuronal activity to cold-stimuli ($15^\circ C$) whereas only 7 glomeruli respond with an increase in neuronal activity to warm stimuli ($30^\circ C$). The majority of the thermosensitive glomeruli is located in the medially oriented half of the antennal lobe. Only 11 of the thermosensitive glomeruli are located at the upper 50 μm from the anterior surface of the



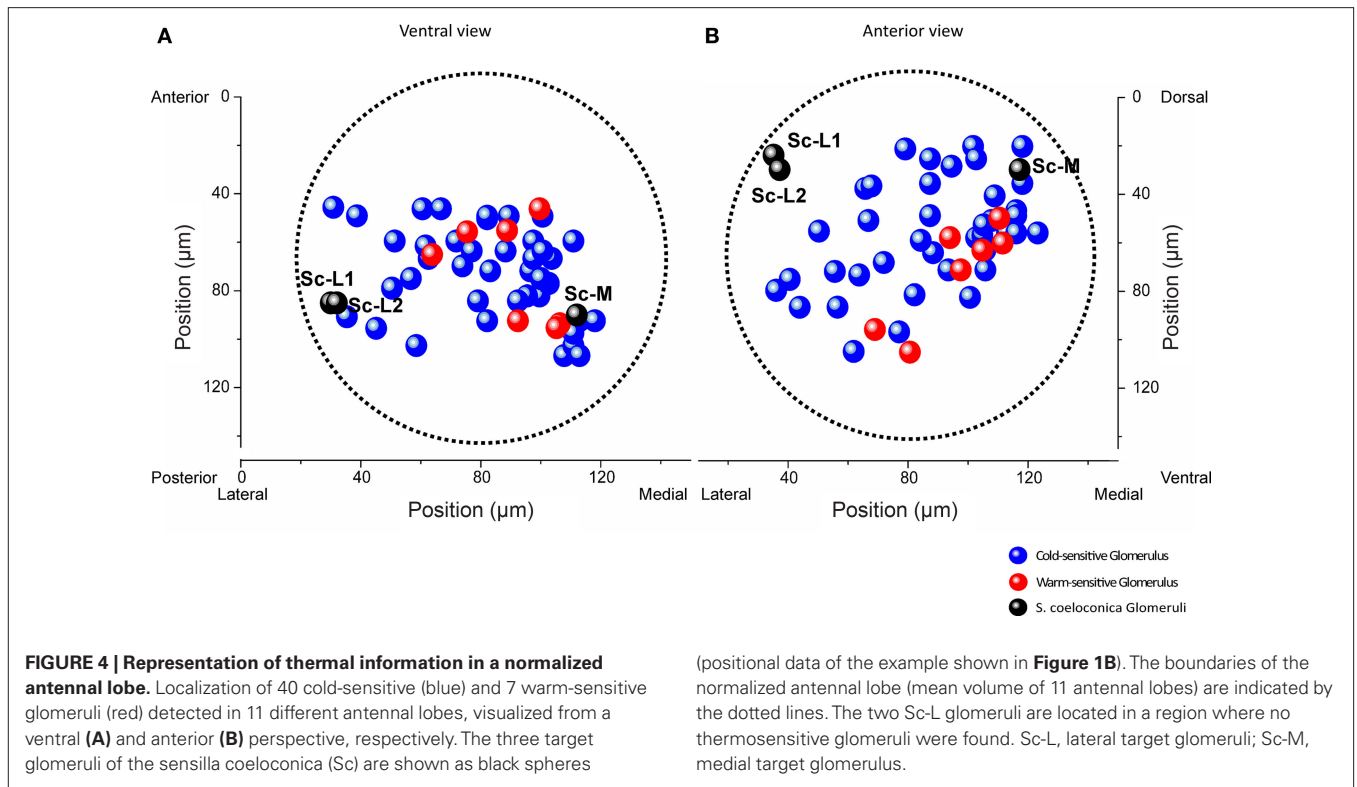
antennal lobe, whereas most of them are located at a depth between 70 and 120 μm ($n = 29$) (ventral view, **Figure 4A**). Among the 47 thermosensitive glomeruli, 8 glomeruli are clustered medially (100–120 μm from the lateral margin, ventral view, **Figure 4A**) at a depth of 80–110 μm along the anterior/posterior axis. This position corresponds to where we also found the Sc-M glomerulus during the single-staining of Sc (ventral view, **Figure 4A**, medial black sphere). Most often (33 times) we detected thermosensitive glomeruli in the dorsal part of the antennal lobe at a distance of approximately 20–80 μm from the dorsal margin (anterior view, **Figure 4B**).

Functional imaging of the Sc target glomeruli

In a number of specimens ($n = 8$) we could identify the Sc-L glomeruli by focusing through the lower (posterior) part of the antennal lobe. We specifically investigated their potential temperature sensitivity in two examples. Our investigations revealed that the Sc-L glomeruli were insensitive to temperature stimuli irrespective of whether warm (30°C) or cold (15°C) temperature changes are presented (**Figures 5A–F**). In **Figure 5A** the two Sc-L glomeruli can

clearly be distinguished. They do not respond to stimulation with cold-stimuli (15°C, green and gray ROIs, depth = 95 μm ; raw data shown in **Figure 5B**, average signal in **Figure 5C**). In the medial part, where the third target glomerulus of the Sc is located (Sc-M glomerulus), we identified two glomeruli as candidates based on their relative position to the Sc-L glomeruli (black and blue ROIs, **Figures 5B,C**). The dorsal glomerulus (black ROI) is stained only weakly. It does not exhibit any substantial activity changes upon temperature stimulation (15°C). However, the second candidate glomerulus (30 μm ventrally, blue ROI) responds with strong oscillations in fluorescence to the applied stimuli (cold-sensitive glomerulus; blue ROI, $\Delta F/F \approx 10\%$).

The second example also shows that the Sc-L glomeruli are not responding to the temperature stimuli (**Figures 5D–F**, 30°C, gray and green ROIs). Considering the raw data traces shown in **Figure 5E** both medial candidate glomeruli respond to the stimulation with warm air in this example (blue ROI, $\Delta F/F \approx 6\%$, black ROI, $\Delta F/F \approx 10\%$). Based on its response characteristics, the ventral glomerulus (blue ROI, **Figure 5D**) classifies as cold-sensitive



glomerulus. The dorsal candidate glomerulus (black ROI, **Figure 5D**) responds to the temperature stimuli slightly differently. During the first stimulus the glomerulus seems to respond as a warm-sensitive glomerulus. However, the response characteristic to the consecutive stimulations classifies this glomerulus as a cold-sensitive one. This is verified by the average signal of the four stimulus trials which shows that the dorsal glomerulus is indeed cold-sensitive (**Figure 5F**, black trace).

Throughout all recordings we never found thermosensitive glomeruli in the area of the antennal lobe where the two Sc-L glomeruli are located (**Figures 4A,B**, black spheres). The correlation of the functional imaging data with the innervation pattern of the Sc provides evidence that the temperature information received by these particular sensilla is sent to the Sc-M glomerulus in the antennal lobe.

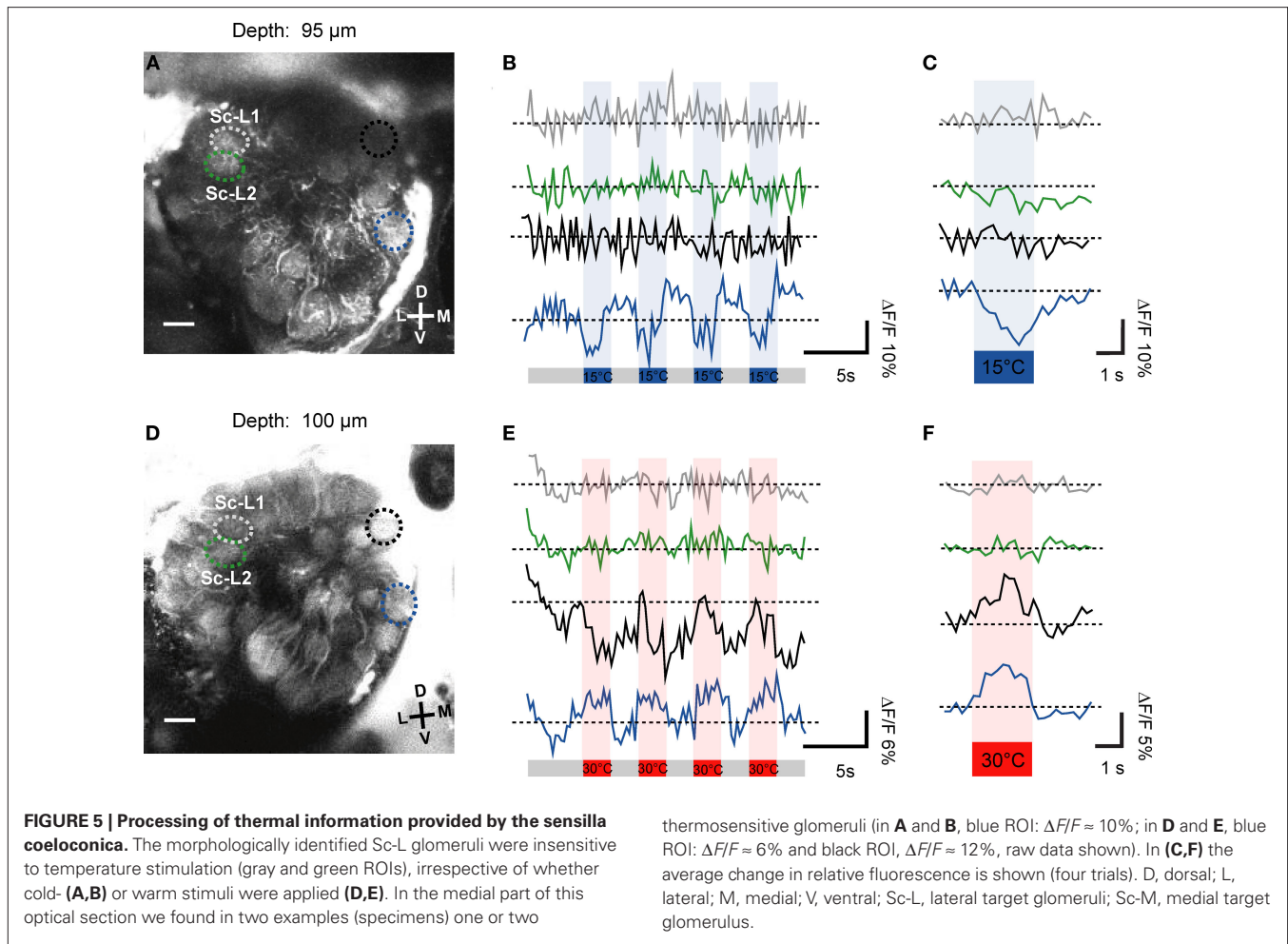
DISCUSSION

In the present study, we show that the receptor neurons of thermosensitive sensilla coeloconica (Sc) project to the first olfactory neuropil, the antennal lobe. Within the antennal lobe, each of the three receptor neuron axons innervates a single glomerulus. Two of the three glomeruli are located side-by-side at a lateral position in the antennal lobe (Sc-L glomeruli), while the third one is located medially. Using two-photon Ca^{2+} imaging of antennal lobe projection neurons, we identified up to 10 thermosensitive glomeruli within a single antennal lobe. We found both warm and cold-sensitive glomeruli, which were mainly located in the medial half of the antennal lobe. The two lateral Sc-L glomeruli targeted by receptor neurons of the Sc are insensitive to temperature stimuli, and we never detected thermosensitive glomeruli

in that specific area of the antennal lobe. In contrast, we found medial thermosensitive glomeruli at the position where the medial target glomerulus (Sc-M glomerulus) was located. Based on these lines of evidence, we conclude that thermal information received by the thermosensitive neuron of the Sc is processed in the Sc-M glomerulus.

CENTRAL PROJECTIONS FROM SENSILLA COELOCONICA

The selective staining of single Sc resulted in three labeled axons, which all projected to the antennal lobe. This number corresponds to the number of receptor neurons identified in a previous study on the fine-structure of the Sc (Ruchty et al., 2009). All three labeled axons densely innervated a single glomerulus each. The three target glomeruli were located in the dorsal part of the ipsilateral antennal lobe at a distance between 80 and 110 μm from its anterior surface (the entire antennal lobe spans approximately 150 μm from anterior to posterior). In the cockroach, the axons of two types of thermosensitive sensilla innervate glomeruli at a similar (dorsal/posterior) region of the antennal lobe, and the thermosensitive neurons (one per sensillum) of both sensilla converge in a single glomerulus (Nishikawa et al., 1995). Electrophysiological recordings in the same species revealed thermosensitive projection- and interneurons in the medial/posterior part of the antennal lobe (Waldow, 1975; Nishikawa et al., 1995; Zeiner and Tichy, 2000; Fischer and Tichy, 2002; Nishino et al., 2003). Studies on the central projections from Sc on the antennae of honeybees (Nishino et al., 2009) and carpenter ants (Nakanishi et al., 2010) suggest similar target regions, although due to the experimental approach used in these two studies, other target region, e.g., the dorsal lobe, cannot be excluded.



Based on the similar position of the target glomeruli of thermosensitive neurons in the leaf-cutting ant and the cockroach, as well as the putative region in the honeybee and the carpenter ant, we assume that in insects in general antennal thermosensitive neurons terminate in specific glomeruli located in similar regions within the antennal lobe. These findings suggest a conserved representation of thermal information in the antennal lobe across insect taxa.

Compared to olfactory sensilla, thermosensitive sensilla occur in low numbers on the antenna of insects (Dumpert, 1972; Tominaga and Yokohari, 1982; Itoh et al., 1984; Hashimoto, 1990; Renthall et al., 2003). In the leaf-cutting ant *Atta vollenweideri* only about 12 Sc have been discovered on each antenna (Ruchty et al., 2009). In olfactory glomeruli it has repeatedly been shown that the size of a glomerulus is related to the number of receptor neuron axons terminating in the glomerulus (Hansson et al., 1995; Berg et al., 1998; Kleineidam et al., 2005; Kelber et al., 2010). The present study shows that the three Sc-glomeruli have a similar volume compared to the adjacent glomeruli, which are targeted by receptor neuron axons from olfactory sensilla (Kelber et al., 2010). Based on the relation between glomerular volume and number of innervating receptor neuron axons, a considerably smaller volume of the Sc-glomeruli would have been expected. To explain our contrasting finding, we hypothesize that the Sc-neurons occupy a larger

volume of their glomeruli because of the larger axon diameters we found, compared to olfactory receptor neurons. This seems to be a common property of receptor neurons associated with Sc in Hymenoptera, since similar results have recently also been shown in honeybees and carpenter ants (Nishino et al., 2009; Nakanishi et al., 2010). Large axon diameters result in fast information propagation and thus may facilitate rapid behavioral responses to, e.g., temperature changes.

FUNCTIONAL ANALYSIS OF THERMOSENSITIVITY IN THE ANTENNAL LOBE

Two-photon Ca^{2+} imaging has so far been applied in insects for physiological studies of the olfactory system in the fruit fly (*Drosophila*; Wang et al., 2003; Suh et al., 2004; Jayaraman and Laurent, 2007; Root et al., 2007; Sachse et al., 2007) and the migratory locust (*Locusta*; Moreaux and Laurent, 2007) as well as of the visual system in the blowfly (*Calliphora*; Haag et al., 2004; Kalb et al., 2004; Kurtz et al., 2006; Spalhoff et al., 2010). In the present study, we use the two-photon microscope for the first time to acquire functional and morphological data of the antennal lobe in a social insect. Compared to conventional imaging, the major advantages of this imaging technique are the reduced dye bleaching and tissue damage and the enhanced imaging depth (Helmchen and Denk, 2005).

These properties allow physiological access to the whole antennal lobe in this ant species. Due to the high *z*-resolution, the 3D reconstruction of single glomeruli and the whole neuropil is possible in parallel to the physiological investigation based on *in vivo* data. This is a major advantage compared to conventional methods like confocal laser scanning microscopy in which the brains have to be dissected and treated with dehydrating chemicals and clearing solutions, in order to obtain morphological data of insect brains or brain neuropils. Especially the dehydration of neuronal tissue leads to shrinking artifacts, which bias volume-based data acquisition (Bucher et al., 2000).

Spatial representation of thermal information in the antennal lobe

We screened the whole antennal lobe volume in search for thermosensitive glomeruli by performing 10–15 consecutive framescans each shifted by 10 μm in *z*-axis. Although we did not quantify the number of glomeruli that were accessible, we are confident that we investigated the great majority of all glomeruli. However, because of the step size chosen (10 μm) it cannot be excluded that we may have missed to record from a small percentage of thermosensitive glomeruli during data acquisition. The mean diameter of the glomeruli in the antennal lobe of *Atta vollenweideri* is about 6.30 μm (Kelber et al., 2010), but an adequate step size to securely capture all glomeruli would have resulted in an experimental protocol exceeding the life time of the preparation. In addition to this experimental limitation, the variances in dye loading of projection neurons possibly resulted in an oversight of thermosensitive glomeruli. Our dye application resulted in some projection neurons loaded heavily with calcium indicator, while others were stained only weakly. Exceedingly high dye concentrations in projection neurons lead to considerable buffering of Ca^{2+} , and weak staining may result in only marginal fluorescence changes. In both cases the applied temperature stimulus may well have elicited neuronal activity changes without causing a measurable change in fluorescence (example **Figure 5B**, black ROI).

Number of thermosensitive glomeruli

The number of thermosensitive glomeruli in the antennal lobe of the leaf-cutting ant possibly reflects the number of different types of thermosensitive neurons in different sensilla on the antenna. Thermosensitive neurons, which differ in their physiological response characteristics are necessary to assess different parameters of the thermal environment, which is a prerequisite for a variety of temperature-guided behaviors. It has recently been shown that the thermosensitive neuron housed in a Sc is extremely sensitive (temperature transients of $\Delta T = 0.005^\circ\text{C}$ can be distinguished), and that the neuron is physiologically adapted to detect rapid and minute temperature changes (Ruchty et al., 2009, 2010). Via sensory adaptation the sensitivity of the neuron is maintained over a wide range of ambient temperatures. Functionally, a role of this sensillum in the thermal landmark learning has been suggested in leaf-cutting ants (Kleineidam et al., 2007; Ruchty et al., 2009, 2010).

Based on the stimulation protocol used in the present study, we were not able to investigate the physiological characteristics of the projection neurons completely, e.g., in terms of adaptation abilities and response characteristics. But our results already show

quite considerable differences in response characteristics between different glomeruli in terms of response latency and response dynamics. This indicates that several thermosensitive neurons with varying physiological characteristics send their axons to antennal lobe glomeruli. It would be of great interest whether the receptor neuron physiology, e.g., of the Sc, predicts the physiology of the projection neuron on which they synapse.

Neurons that do not adapt as strongly as the thermosensitive neurons of Sc, thereby providing the animals with information about the actual ambient temperature in their surrounding, have been described in antennal sensilla of the migratory locust *Locusta migratoria* (Waldow, 1970; Ameismeier and Loftus, 1988), the cockroach *Periplaneta americana* (Nishikawa et al., 1992) and the honeybee *Apis mellifera* (Lacher, 1964). In ants, neurons with such non-adapting physiological characteristics are expected as well, since ants can assess and respond to steady temperatures with very high accuracy, e.g., during brood care (Roces and Núñez, 1989, 1995; Weidenmüller et al., 2009). Possible candidate sensilla to house thermosensitive neurons with that particular physiological characteristics are the sensilla coelocapitula (Yokohari, 1983). We assume that these putative antennal thermosensitive sensilla send their axons to the antennal lobe as well.

In 11 different individuals we found a total of 47 thermosensitive glomeruli with a maximum of 10 in a single antennal lobe. Although most of the discovered glomeruli were cold-sensitive glomeruli, which responded with increasing neuronal activity to negative temperature steps, we also found a couple of warm-sensitive glomeruli ($n = 7$). Due to the fact that each neuron is, at least to some extent, sensitive to temperature stimuli and increases its neuronal activity with increasing temperature, we cannot exclude unspecific temperature responses for the warm-sensitive glomeruli discovered here.

Apart from unspecific thermosensitivity there are several other possibilities which could potentially result in warm-sensitive glomeruli. The most obvious explanation is that warm-sensitive receptor neurons occur in addition to the already discovered cold-sensitive ones on the antennae. Warm-sensitive antennal neurons were discovered, but not further investigated, in a closely related leaf-cutting ant species (Kleineidam and Tautz, 1996). Furthermore, the presence of warm-sensitive projection neurons as discovered in the present study does not necessarily require warm-sensitive receptor neurons in the periphery. In the cockroach, warm-sensitive projection neurons and interneurons were found, although no antennal warm-sensitive neurons have been discovered there so far (Nishikawa et al., 1995; Zeiner and Tichy, 2000; Fischer and Tichy, 2002). Fischer and Tichy (2002) speculated that the response of warm-sensitive projection neurons was the result of the antennal lobe network, where the input from cold-sensitive receptor neurons to their target glomeruli may lead to a disinhibition of other glomeruli and hence to inverted response characteristics (Fischer and Tichy, 2002).

A further plausible explanation could be that the respective projection neurons are not at all driven by antennal neurons but rather excited via central thermosensitive neurons comparable to the recently discovered warm-sensitive anterior cell neurons involved in thermoregulation in *Drosophila* (Hamada et al., 2008). Whether the recorded increase of

neuronal activity in projection neurons to warm stimuli is the result of neuronal activity in a peripheral or a central thermosensitive neuron or whether the neuronal network within the antennal lobe triggers the response has to be shown in future experiments.

Processing of thermal information provided by sensilla coeloconica

The comparison of the receptor neuron staining and the Ca²⁺ imaging experiments led us to conclude that the thermosensitive neuron of the Sc innervates the Sc-M glomerulus. Three lines of evidence allow this conclusion. (1) The screening of the antennal lobe for thermosensitive glomeruli clearly showed that the area where the two Sc-L glomeruli are located is spared by thermosensitive glomeruli, and (2) that thermal information is mainly processed within the medial part of the neuropil where we found in six specimens a single cold-sensitive glomerulus, closely located to the position of the Sc-M glomerulus (Figures 4A,B). (3) Our conclusion is further supported by the functional imaging data of the two Sc-L glomeruli, which did not exhibit any sensitivity to thermal stimuli (Figures 5A–F). Unfortunately, we could not identify the medial Sc-glomerulus unambiguously during the experiments. Using the Sc-L glomeruli as landmarks, we identified two cold-sensitive candidate glomeruli of which one is supposed to be the target of the Sc thermosensitive neuron (Sc-M glomerulus) (Figures 5A–F).

REFERENCES

- Altner, H., and Loftus, R. (1985). Ultrastructure and function of insect thermoreceptors and hygroreceptors. *Annu. Rev. Entomol.* 30, 273–295.
- Altner, H., Routil, C., and Loftus, R. (1981). The structure of bimodal chemoreceptive, thermoreceptive, and hygroreceptive sensilla on the antenna of *Locusta migratoria*. *Cell Tissue Res.* 215, 289–308.
- Altner, H., Sass, H., and Loftus, I. (1977). Relationship between structure and function of antennal chemoreceptive, hygroreceptive, and thermoreceptive sensilla in *Periplaneta americana*. *Cell Tissue Res.* 176, 389–405.
- Ameismeier, F., and Loftus, R. (1988). Response characteristics of cold cell on the antenna of *Locusta migratoria* L. *J. Comp. Physiol. A* 163, 507–516.
- Berg, B. G., Almaas, T. J., Bjaalie, J. G., and Mustaparta, H. (1998). The macroglomerular complex of the antennal lobe in the tobacco budworm moth *Heliothis virescens*: specified subdivision in four compartments according to information about biologically significant compounds. *J. Comp. Physiol. A* 183, 669–682.
- Bucher, D., Scholz, M., Stetter, M., Obermayer, K., and Pflüger, H. J. (2000). Correction methods for three-dimensional reconstructions from confocal images: I. Tissue shrinking and axial scaling. *J. Neurosci. Methods* 100, 135–143.
- Davis, E. E. (1977). Response of antennal receptors of male *Aedes aegypti* mosquito. *J. Insect Physiol.* 23, 613–617.
- Dumpert, K. (1978). Das Sozialleben der Ameisen. Berlin, Hamburg: Verlag Paul Parey.
- Dumpert, K. (1972). Structure and distribution of sensilla on antennal flagellum of *Lasius fuliginosus* (Latreille) (Hymenoptera, Formicidae). *Z. Morphol. Tiere* 73, 95–116.
- Dupuy, F., Josens, R., Giurfa, M., and Sandoz, J. C. (2010). Calcium imaging in the ant *Camponotus fellah* reveals a conserved odour-similarity space in insects and mammals. *BMC Neurosci.* 26, 11–28.
- Evans, W. G. (1964). Infra-red receptors in *Melanophila acuminata* Degeer. *Nature* 202, 211.
- Fischer, H., and Tichy, H. (2002). Cold-receptor cells supply both cold- and warm-responsive projection neurons in the antennal lobe of the cockroach. *J. Comp. Physiol. A* 188, 643–648.
- Galizia, C. G., and Rössler, W. (2010). Parallel olfactory systems in insects: anatomy and function. *Annu. Rev. Entomol.* 55, 399–420.
- Grynkiewicz, G., Poenie, M., and Tsien, R. Y. (1985). A new generation of Ca²⁺ indicators with greatly improved fluorescence properties. *J. Biol. Chem.* 260, 3440–3450.
- Haag, J., Denk, W., and Borst, A. (2004). Fly motion vision is based on Reichardt detectors regardless of the signal-to-noise ratio. *Proc. Natl. Acad. Sci. U.S.A.* 101, 16333–16338.
- Hamada, F. N., Rosenzweig, M., Kang, K., Pulver, S. R., Ghezzi, A., Jegla, T. J., and Garrity, P. A. (2008). An internal thermal sensor controlling temperature preference in *Drosophila*. *Nature* 454, 217–255.
- Hansson, B. S., Almaas, T. J., and Anton, S. (1995). Chemical communication in heliothine moths: 5. Antennal lobe projection patterns of pheromone-detecting olfactory receptor neurons in the male *Heliothis virescens* (Lepidoptera, Noctuidae). *J. Comp. Physiol. A* 177, 535–543.
- Hansson, B. S., Ochieng, S. A., Grosmaître, X., Anton, S., and Njagi, P. G. N. (1996). Physiological responses and central nervous projections of antennal olfactory receptor neurons in the adult desert locust, *Schistocerca gregaria* (Orthoptera: Acrididae). *J. Comp. Physiol. A* 179, 157–167.
- Hashimoto, Y. (1990). Unique features of sensilla on the antennae of formicidae (Hymenoptera). *Appl. Entomol. Zool.* 25, 491–501.
- Helmchen, F., and Denk, W. (2005). Deep tissue two-photon microscopy. *Nat. Methods* 2, 932–940.
- Itoh, T., Yokohari, F., and Tominaga, Y. (1984). 2 types of antennal hygroreceptive and thermoreceptive sensilla of the cricket, *Gryllus bimaculatus* (De Geer). *Zool. Sci.* 1, 533–543.
- Jayaraman, V., and Laurent, G. (2007). Evaluating a genetically encoded optical sensor of neural activity using electrophysiology in intact adult fruit flies. *Front. Neural Circuits* 1:3. doi: 10.3389/neuro.04/003.2007.
- Kalb, J., Nielsen, T., Fricke, M., Egelhaaf, M., and Kurtz, R. (2004). In vivo two-photon laser-scanning microscopy of Ca²⁺ dynamics in visual motion-sensitive neurons. *Biochem. Biophys. Res. Commun.* 316, 341–347.
- Kelber, C., Rössler, W., and Kleineidam, C. J. (2010). Phenotypic plasticity in number of glomeruli and sensory innervation of the antennal lobe in leaf-cutting ant workers (*A. vollenweideri*). *Dev. Neurobiol.* 70, 222–234.
- Kirschner, S., Kleineidam, C. J., Zube, C., Rybak, J., Grünewald, B., and Rössler, W. (2006). Dual olfactory pathway in the honeybee, *Apis mellifera*. *J. Comp. Neurol.* 499, 933–952.
- Kleineidam, C., and Tautz, J. (1996). Perception of carbon dioxide and other “air-condition” parameters in the leaf cutting ant *Atta cephalotes*. *Naturwissenschaften* 83, 566–568.
- Kleineidam, C. J., Obermayer, M., Halbach, W., and Rössler, W. (2005). A macroglomerulus in the antennal lobe of leaf-cutting ant workers and its possible functional significance. *Chem. Senses* 30, 383–392.
- Kleineidam, C. J., Ruchty, M., Casero-Montes, Z. A., and Roces, F. (2007). Thermal radiation as a learned orientation cue in leaf-cutting ants (*Atta vollenweideri*). *J. Insect Physiol.* 53, 478–487.
- Kuebler, L., Kelber, C., and Kleineidam, C. (2010). Distinct antennal lobe

- phenotypes in the leaf-cutting ant (*Atta vollenweideri*). *J. Comp. Neurol.* 518, 352–365.
- Kurtz, R., Fricke, M., Kalb, J., Tinnefeld, P., and Sauer, M. (2006). Application of multiline two-photon microscopy to functional *in vivo* imaging. *J. Neurosci. Methods* 151, 276–286.
- Lacher, V. (1964). Elektrophysiologische Untersuchungen an Einzelnen Rezeptoren für Geruch, Kohlendioxyd, Luftfeuchtigkeit und Temperatur auf den Antennen der Arbeitsbiene und der Drohne (*Apis mellifica* L.). *Z. Vgl. Physiol.* 48, 587–623.
- Lazzari, C. R. (2009). Orientation towards hosts in haematophagous insects: an integrative perspective. *Adv. Insect Physiol.* 37, 1–58.
- Lazzari, C. R., and Núñez, J. A. (1989). The response to radiant heat and the estimation of the temperature of distant sources in *Triatoma infestans*. *J. Insect Physiol.* 35, 525–529.
- Mobbs, P. G. (1982). The brain of the honeybee *Apis mellifera*. 1. The connections and spatial organization of the mushroom bodies. *Philos. Trans. R. Soc. Lond., B, Biol. Sci.* 298, 309–354.
- Moreaux, L., and Laurent, G. (2007). Estimating firing rates from calcium signals in locust projection neurons *in vivo*. *Front. Neural Circuits* 1:2. doi: 10.3389/neuro.04/002.2007.
- Nakanishi, A., Nishino, H., Watanabe, H., Yokohari, F., and Nishikawa, M. (2010). Sex-specific antennal sensory system in the ant *Camponotus japonicus*: glomerular organizations of antennal lobes. *J. Comp. Neurol.* 518, 2186–2201.
- Nishikawa, M., Yokohari, F., and Ishibashi, T. (1992). Response characteristics of 2 types of cold receptors on the antennae of the cockroach, *Periplaneta americana* L. *J. Comp. Physiol. A* 171, 299–307.
- Nishikawa, M., Yokohari, F., and Ishibashi, T. (1995). Central projections of the antennal cold receptor neurons and hygroreceptor neurons of the cockroach *Periplaneta americana*. *J. Comp. Neurol.* 361, 165–176.
- Nishino, H., Nishikawa, M., Mizunami, M., and Yokohari, F. (2009). Functional and topographic segregation of glomeruli revealed by local staining of antennal sensory neurons in the honeybee *Apis mellifera*. *J. Comp. Neurol.* 515, 161–180.
- Nishino, H., Yamashita, S., Yamazaki, Y., Nishikawa, M., Yokohari, F., and Mizunami, M. (2003). Projection neurons originating from thermo- and hygroreceptive glomeruli in the antennal lobe of the cockroach. *J. Comp. Neurol.* 455, 40–55.
- Renthal, R., Velasquez, D., Olmos, D., Hampton, J., and Wergin, W. P. (2003). Structure and distribution of antennal sensilla of the red imported fire ant. *Micron* 34, 405–413.
- Roces, F., and Núñez, J. A. (1989). Brood translocation and circadian variation of temperature preference in the ant *Camponotus mus*. *Oecologia* 81, 33–37.
- Roces, F., and Núñez, J. A. (1995). Thermal sensitivity during brood care in workers of 2 *Camponotus* ant species – circadian variation and its ecological correlates. *J. Insect Physiol.* 41, 659–669.
- Root, C. M., Semmelhack, J. L., Wong, A. M., Flores, J., and Wang, J. W. (2007). Propagation of olfactory information in *Drosophila*. *Proc. Natl. Acad. Sci. U.S.A.* 104, 11826–11831.
- Ruchty, M., Roces, F., and Kleineidam, C. J. (2010). Detection of minute temperature transients by thermosensitive neurons in ants. *J. Neurophysiol.* 104, 1249–1256.
- Ruchty, M., Romani, R., Kuebler, L. S., Ruschioni, S., Roces, F., Isidoro, N., and Kleineidam, C. J. (2009). The thermo-sensitive sensilla coeloconica of leaf-cutting ants (*Atta vollenweideri*). *Arthropod Struct. Dev.* 38, 195–205.
- Sachse, S., and Galizia, C. G. (2002). Role of inhibition for temporal and spatial odor representation in olfactory output neurons: a calcium imaging study. *J. Neurophysiol.* 87, 1106–1117.
- Sachse, S., Rueckert, E., Keller, A., Okada, R., Tanaka, N. K., Ito, K., and Vosshall, L. B. (2007). Activity-dependent plasticity in an olfactory circuit. *Neuron* 56, 838–850.
- Schmitz, H., Bleckmann, H., and Murtz, M. (1997). Infrared detection in a beetle. *Nature* 386, 773–774.
- Schmitz, H., Trenner, S., Hofmann, M. H., and Bleckmann, H. (2000). The ability of *Rhodnius prolixus* (Hemiptera; Reduviidae) to approach a thermal source solely by its infrared radiation. *J. Insect Physiol.* 46, 745–751.
- Spalhoff, C., Egelhaaf, M., Tinnefeld, P., and Kurtz, R. (2010). Localized direction selective responses in the dendrites of visual interneurons of the fly. *BMC Biol.* 8, 36.
- Suh, G. S. B., Wong, A. M., Hergarden, A. C., Wang, J. W., Simon, A. F., Benzer, S., Axel, R., and Anderson, D. J. (2004). A single population of olfactory sensory neurons mediates an innate avoidance behaviour in *Drosophila*. *Nature* 431, 854–859.
- Tichy, H. (1979). Hygro- and thermoreceptive triad in antennal sensillum of the stick insect, *Carausius morosus*. *J. Comp. Physiol. A* 132, 149–152.
- Tominaga, Y., and Yokohari, F. (1982). External structure of the sensillum capitulum, a hygroreceptive and thermoreceptive sensillum of the cockroach, *Periplaneta americana*. *Cell Tissue Res.* 226, 309–318.
- Vondran, T., Apel, K. H., and Schmitz, H. (1995). The infrared receptor of *Melanophila acuminata* De Geer (Coleoptera: Buprestidae): ultrastructural study of a unique insect thermoreceptor and its possible descent from a hair mechanoreceptor. *Tissue Cell* 27, 645–658.
- Waldow, U. (1970). Electrophysiological investigations of moist, dry and cold receptors on antenna of migratory locust. *Z. Vgl. Physiol.* 69, 249–283.
- Waldow, U. (1975). Multimodal neurons in the deutocerebrum of *Periplaneta americana*. *J. Comp. Physiol.* 101, 329–341.
- Wang, J. W., Wong, A. M., Flores, J., Vosshall, L. B., and Axel, R. (2003). Two-photon calcium imaging reveals an odor-evoked map of activity in the fly brain. *Cell* 112, 271–282.
- Weidenmüller, A., Mayr, C., Kleineidam, C. J., and Roces, F. (2009). Preimaginal and adult experience modulates the thermal response behavior of ants. *Curr. Biol.* 19, 1897–1902.
- Yokohari, F. (1983). The coelocapitular sensillum, an antennal hygroreceptive and thermoreceptive sensillum of the honey bee, *Apis mellifera*. *Cell Tissue Res.* 233, 355–365.
- Zeiner, R., and Tichy, H. (2000). Integration of temperature and olfactory information in cockroach antennal lobe glomeruli. *J. Comp. Physiol. A* 186, 717–727.
- Zube, C., Kleineidam, C. J., Kirschner, S., and Rössler, W. (2008). Organization of the olfactory pathway and odor processing in the antennal lobe of the ant *Camponotus floridanus*. *J. Comp. Neurol.* 506, 425–441.

Conflict of Interest Statement: The authors declare that the research was conducted in the absence of any commercial or financial relationships that could be construed as a potential conflict of interest.

Received: 10 September 2010; accepted: 27 October 2010; published online: 15 November 2010.

Citation: Ruchty M, Helmchen F, Wehner R and Kleineidam CJ (2010) Representation of thermal information in the antennal lobe of leaf-cutting ants. *Front. Behav. Neurosci.* 4:174. doi: 10.3389/fnbeh.2010.00174
Copyright © 2010 Ruchty, Helmchen, Wehner and Kleineidam. This is an open-access article subject to an exclusive license agreement between the authors and the Frontiers Research Foundation, which permits unrestricted use, distribution, and reproduction in any medium, provided the original authors and source are credited.